Chemical Engineering Science 147 (2016) 30–46

Contents lists available at ScienceDirect

Chemical Engineering Science

journal homepage: www.elsevier.com/locate/ces

Global optimization of heat exchanger networks using a new generalized superstructure

Sung Young Kim, Miguel Bagajewicz *

School of Chemical Engineering and Material Science, University of Oklahoma, 100 East Boyd Street, T-335, Norman, OK 73019-0628, USA

HIGHLIGHTS

- We extend the general HEN superstructure proposed by Floudas et al., 1986.
- we compare two different reformulations, and we solve the problem globally.
- We introduce a new feature to RYSIA, the global optimizer we developed recently, called lifting partitioning.
- Among results, we obtain structures that cannot be obtained using other models (stages, etc.).

ARTICLE INFO

Article history:
Received 9 July 2015
Received in revised form
7 January 2016
Accepted 2 February 2016
Available online 9 February 2016

Keywords:
Heat exchanger networks
Global optimization
RYSIA
Generalized superstructure

ABSTRACT

We present an extension of a previously presented superstructure (Floudas et al., 1986) for heat exchanger network grassroots design. This extension is such that it includes several matches between two streams, activates splitting control and allows for mixing temperature control. We solve this model globally using RYSIA, a recently developed method bound contraction procedure (Faria and Bagajewicz, 2011a, 2011b, 2011c; Faria et al., 2015). We also add a new RYSIA feature called Lifting Partitioning. Results show structures that cannot be obtained using the stages model (Yee and Grossmann, 1990) or other similar restrictive models.

1. Introduction

The problem of designing heat exchanger networks is perhaps the oldest problem in the discipline of Process Synthesis/Process Systems Engineering. Many articles were published and continue to be published because, arguably, the problem continues to challenge academia and practitioners.

The latest good review is an annotated bibliography by Furman and Sahinidis (2002). Of all this work, we specifically point to a general superstructure for HEN design was presented by Floudas et al. (1986), which is the starting point of our work. It consisted of a model that included one heat exchanger between every hot and cold stream, with connections made such that every possible flowsheet is represented in the superstructure. The model, however, was not used in practice for a variety of reasons. First, the MINLP solvers of the time, and many of them today, do not have good enough feasibility steps that would guarantee at least one local minimum (the model is non-convex) and without good initial points it usually turns infeasible. This discouraged researchers and practitioners. Second, the model would render some impractical answers, product of several splitting and mixing (we illustrate this later in this article). Third, many systems that exhibit heat transfer bottlenecks (i.e. pinches), require that some pairs of streams exchange heat in more than one exchanger, typically two (one exchanger on each side of the pinch, not consecutively, of course).

As a response to the aforementioned difficulties, a model more amenable to MINLP solvers was proposed (Yee and Grossmann, 1990), which makes a series of assumptions: it assumes isothermal mixing and presents several stages where more than one match between streams takes place. What made the model attractive is that the only nonlinearity could be confined to the objective function. The model became very popular, to the point that some other studies followed not assuming isothermal mixing (Björk and Weterlund, 2002) and allowing some different configurations (Huang and Karimi, 2013). All these efforts were not able to capture some alternative structures, like several exchangers in series on each branch of each stage. Thus, the only model that is still capable of capturing important and useful alternatives is a

* Corresponding author. Tel.: +1 405 325 5458.
E-mail address: bagajewicz@ou.edu (M. Bagajewicz).

http://dx.doi.org/10.1016/j.ces.2016.02.002
0009-2509/

generalized superstructure where several exchangers between two streams can be used.

As stated, the major difficulty of all the aforementioned models is the high level of non-convexity of the MINLP models, which not only leads to local optima, but may also fail to produce a feasible answer if it is not provided with good initial points. The only alternative to these models is the use of global optimization.

The academic efforts and the available commercial software were reviewed in our previous article (Faria et al., 2015). We only highlight what are the options we pursue in this article: all HEN models contain bilinear terms consisting of flowrates multiplied by temperatures. In addition, for HEN models, the heat transfer equations relating heat transferred with LMTD values are nonconvex. If one uses some rational approximations (Paterson, 1984; Chen, 1987), one can make appropriate substitutions (Manousiouthakis and Sourlas, 1992), to reformulate the problem using as one containing purely quadratic/bilinear models.

In this article, we explore the use of our bound contraction procedure for global optimization (Faria and Bagajewicz, 2011a). In our lower bound, we follow the direct partitioning procedure 1 (DPP1) strategy for the relaxation of bilinear terms and we exploit the univariate nature of the LMTD terms (or their rational equivalents), to build relaxations that do not require the addition of new variables (Faria et al., 2015). Finally, we also use a new concept of partitioning additional variables that help "lift" the value of the lower bound. We call the technique Lifting Partitioning.

The paper is organized as follows: we present the revised superstructure model first, including mixing and splitting control constraints. We follow with the lower bound model. We discuss the bound contraction strategy next, including the lifting partitioning and the uneven interval size bound contraction procedure. We then present results.

2. Generalized superstructure

The HEN design model of the heat exchanger network uses the superstructure model developed by Floudas et al. (1986). In order to describe how the HEN design model can be developed, we address a simple network, which has one hot stream and two cold streams in Fig. 1. Without loss of generality, we assume there are two heat exchangers per hot/cold stream match and they are not necessarily contiguous or in series. Fig. 1 illustrates the nature of the superstructure for just one hot stream and two cold streams and two exchangers per pair of streams, although the model can have many exchangers.

In the original formulation by Floudas et al. (1986) the feasible space is defined by nonlinear constraints, many of which are bilinear, and other purely nonconvex functions. Bilinear functions are included in the heat balances equations of heat exchangers and mixers. Nonconvex functions are the part of heat exchanger area calculations. The non-convex and bilinear MINLP model presented in this paper differs slightly from the original formulation.

We first introduce the nomenclature for streams. They are depicted in Fig. 2. Index i refers to hot stream and j to cold stream. Each exchanger k has their inlet and outlet temperatures and flowrates denoted by $Th^{i,j,k}_{hx-in}$, $Th^{i,j,k}_{hx-out}$, $Fh^{i,j,k}_{hx-in}$ and $Fh^{i,j,k}_{hx-out}$, respectively. These inlet temperatures and flowrates are a product of mixing a portion of the feed $Fh^{i,j,k}_{in}$ with streams from other exchangers (i,jj,kk), $fh^{i,jj,j}_{kk,k}$. The variable $fh^{i,j,jj}_{k,kk}$ represents the hot stream from the heat exchanger (i,j,k) to split to the heat exchanger (i,jj,kk). If kk is greater than k, there is no stream from the heat exchanger (i,j,k) to (i,jj,kk).

We now present the equations of the model:

- *Mass balances for splitters*

$$F_i - \sum_j \sum_k Fh^{i,j,k}_{in} = 0 \quad \forall i \tag{1}$$

$$F_j - \sum_i \sum_k Fc^{i,j,k}_{in} = 0 \quad \forall j \tag{2}$$

$$Fh^{i,j,k}_{hx-out} - \left(\sum_{jj} \sum_{kk} fh^{i,j,jj}_{k,kk} + Fh^{i,j,k}_{out} \right) = 0 \quad (k \le kk) \quad \forall i,j,k \tag{3}$$

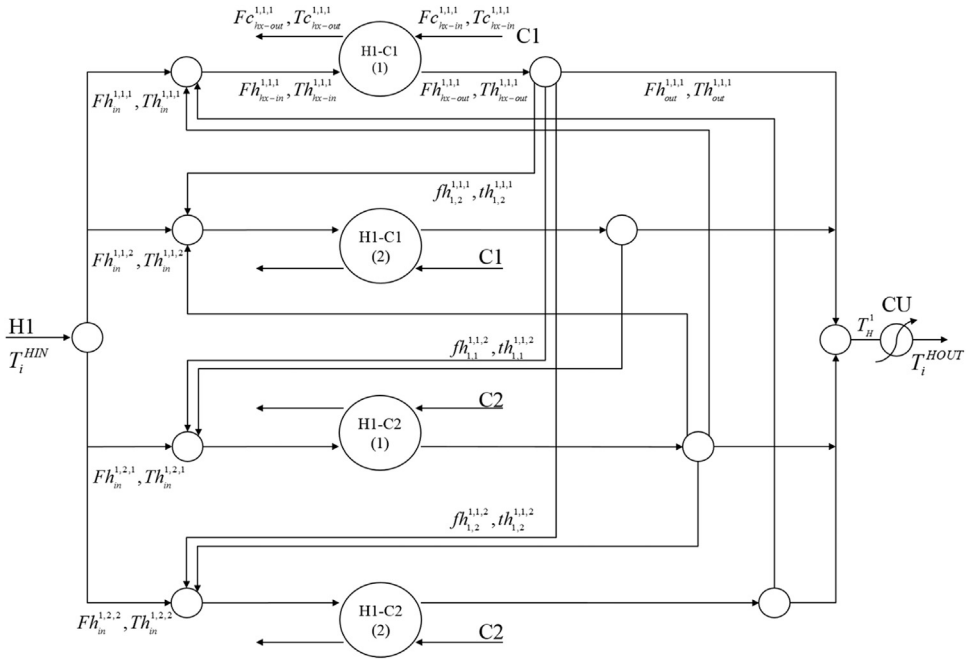

Fig. 1. Heat exchanger network superstructure; two exchangers per match.

$$Fc_{hx-out}^{i,j,k} - \left(\sum_{ii} \sum_{kk} fc_{k,kk}^{i,i,ii} + Fc_{out}^{i,j,k} \right) = 0 \quad (k \le kk) \quad \forall i,j,k \tag{4}$$

- *Mass balances for mixers*

$$Fh_{in}^{i,j,k} + \sum_{jj} \sum_{kk} fh_{kk,k}^{i,jj,j} - Fh_{hx-in}^{i,j,k} = 0 \quad (k \ge kk) \quad \forall i,j,k \tag{5}$$

$$Fc_{in}^{i,j,k} + \sum_{ii} \sum_{kk} fc_{kk,k}^{i,ii,i} - Fc_{hx-in}^{i,j,k} = 0 \quad (k \ge kk) \quad \forall i,j,k \tag{6}$$

- *Heat balances for mixers*

$$F_i T_H^i - \sum_j \sum_k Fh_{out}^{i,j,k} Th_{out}^{i,j,k} = 0 \quad \forall i \tag{7}$$

$$F_j T_C^j - \sum_i \sum_k Fc_{out}^{i,j,k} Tc_{out}^{i,j,k} = 0 \quad \forall j \tag{8}$$

$$Fh_{in}^{i,j,k} Th_{in}^{i,j,k} + \sum_{jj} \sum_{kk} fh_{kk,k}^{i,jj,j} th_{kk,k}^{i,jj,j} - Fh_{hx-in}^{i,j,k} Th_{hx-in}^{i,j,k} = 0 \quad (k \ge kk) \quad \forall i,j,k \tag{9}$$

$$Fc_{in}^{i,j,k} Tc_{in}^{i,j,k} + \sum_{ii} \sum_{kk} fc_{kk,k}^{i,ii,i} tc_{kk,k}^{j,ii,i} - Fc_{hx-in}^{i,j,k} Tc_{hx-in}^{i,j,k} = 0 \quad (k \ge kk) \quad \forall i,j,k \tag{10}$$

- *Heat balances for heat exchangers*

$$Q_{i,j,k} - Fh_{hx-in}^{i,j,k} \left(Th_{hx-in}^{i,j,k} - Th_{hx-out}^{i,j,k} \right) = 0 \quad \forall i,j,k \tag{11}$$

$$Q_{i,j,k} - Fc_{hx-in}^{i,j,k} \left(Tc_{hx-in}^{i,j,k} - Tc_{hx-out}^{i,j,k} \right) = 0 \quad \forall i,j,k \tag{12}$$

- *Overall heat balances for each stream* (*we assume the utilities are last*)

$$F_i \left(T_i^{HIN} - T_i^{HOUT} \right) = \sum_j \sum_k Q_{i,j,k} + Q_i^{CU} \quad \forall i \tag{13}$$

$$F_j \left(T_j^{COUT} - T_j^{CIN} \right) = \sum_i \sum_k Q_{i,j,k} + Q_j^{HU} \quad \forall j \tag{14}$$

- *Hot and cold utility load*

$$Q_i^{CU} = F_i \left(T_H^i - T_i^{HOUT} \right) \quad \forall i \tag{15}$$

$$Q_j^{HU} = F_j \left(T_j^{COUT} - T_C^j \right) \quad \forall j \tag{16}$$

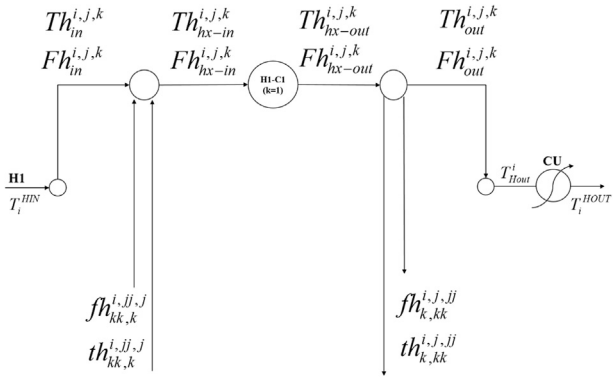

Fig. 2. Stream nomenclatures for temperatures and flowrates.

- *Logical constraints*

$$Q_{i,j} - \Omega Z_{i,j} \le 0 \quad \forall i,j,k \tag{17}$$

$$Q_i^{CU} - \Omega Z_i^{CU} \le 0 \quad \forall i \tag{18}$$

$$Q_j^{HU} - \Omega Z_j^{HU} \le 0 \quad \forall j \tag{19}$$

The value of Ω used is $\Omega = F_j \left(T_j^{COUT} - T_j^{CIN} \right)$.

- *Approach temperature*

$$\Delta Th_{i,j,k} \le Th_{hx-in}^{i,j,k} - Tc_{hx-out}^{i,j,k} + \Gamma \left(1 - Z_{i,j,k} \right) \quad \forall i,j,k \tag{20}$$

$$\Delta Tc_{i,j,k} \le Th_{hx-out}^{i,j,k} - Tc_{hx-in}^{i,j,k} + \Gamma \left(1 - Z_{i,j,k} \right) \quad \forall i,j,k \tag{21}$$

$$\Delta T_i^{CU} \le T_H^i - T_{OUT,CU} + \Gamma \left(1 - Z_i^{CU} \right) \quad \forall i \tag{22}$$

$$\Delta T_j^{HU} \le T_{OUT,HU} - T_C^j + \Gamma \left(1 - Z_j^{HU} \right) \quad \forall j \tag{23}$$

The value of Ω used is $\Omega = F_j \left(T_j^{COUT} - T_j^{CIN} \right)$.

- *Minimum temperature approach*

$$\Delta Th_{i,j,k} \ge EMAT_{i,j} \quad \forall i,j,k \tag{24}$$

$$\Delta Tc_{i,j,k} \ge EMAT_{i,j} \quad \forall i,j,k \tag{25}$$

$$\Delta T_i^{CU} \ge EMAT_{i,j} \quad \forall i \tag{26}$$

$$\Delta T_j^{HU} \ge EMAT_{i,j} \quad \forall j \tag{27}$$

- *Equality of temperatures in splitters* (*inlet and outlet temperatures*)

$$Th_{in}^{i,j,k} = T_i^{HIN} \quad \forall i,j,k \tag{28}$$

$$Tc_{in}^{i,j,k} = T_j^{CIN} \quad \forall i,j,k \tag{29}$$

$$Th_{hx-out}^{i,j,k} = Th_{out}^{i,j,k} = th_{k,kk}^{i,j,jj} \quad \forall i,j,k \tag{30}$$

$$Tc_{hx-out}^{i,j,k} = Tc_{out}^{i,j,k} = tc_{k,kk}^{j,i,ii} \quad \forall i,j,k \tag{31}$$

Additional constraints for temperature (when $T_i^{HIN} \le T_j^{COUT}$ or $T_i^{HOUT} \le T_j^{CIN}$)

$$T_j^{CIN} + EMAT_{i,j} \le Th_{hx-in}^{i,j,k} \le T_i^{HIN} \quad \forall i,j,k \tag{32}$$

$$T_j^{CIN} \le Tc_{hx-in}^{i,j,k} \le T_i^{HIN} - EMAT_{i,j} \quad \forall i,j,k \tag{33}$$

$$\max \left(T_j^{CIN} + EMAT_{i,j}, T_i^{HOUT} \right) \le Th_{hx-out}^{i,j,k} \le T_i^{HIN} \quad \forall i,j,k \tag{34}$$

$$\max \left(T_i^{HOUT} - \left(T_i^{HIN} - T_j^{CIN} \right), T_j^{CIN} \right) \le Tc_{hx-out}^{i,j,k} \le \min \left(T_i^{HIN} - EMAT_{i,j}, T_j^{COUT} \right) \quad \forall i,j,k \tag{35}$$

$$\max \left(T_j^{CIN} + EMAT_{i,j}, T_i^{HOUT} \right) \le thh_{k,kk}^{i,j,jj} \le T_i^{HIN} \quad \forall i,j,jj,k,kk \tag{36}$$

$$\max \left(T_i^{HOUT} - \left(T_i^{HIN} - T_j^{CIN} \right), T_j^{CIN} \right) \le tcc_{k,kk}^{j,i,ii} \le \min \left(T_i^{HIN} - EMAT_{i,j}, T_j^{COUT} \right) \quad \forall i,ii,j,k,kk \tag{37}$$

The value of EMAT can be chosen for each match, but in industrial practices, usually two values are used, one for non-phase change fluids and one for exchangers where phase changes (condensers, etc.). The minimum values also change depending on the type of

exchanger used (shell and tube, plate, etc.).
These constraints are needed when $T_i^{HIN} \le T_j^{COUT}$ or $T_i^{HOUT} \le T_j^{CIN}$, so that better bounds on temperatures are used. We believe this helps computations.

- *Limitation to avoid recycling*

We avoid the recycle crossed out in Fig. 3. Specifically, when the flow form one exchanger to another is positive, then the flow back is forbidden. This helps computationally.

$$\sum_{k,kk} fh_{k,kk}^{i,j,jj} - Ymh_{i,j,jj} \cdot \Gamma \le 0 \quad (j \ne jj) \quad \forall i,j,jj \tag{38}$$

$$\sum_{k,kk} fh_{k,kk}^{i,jj,j} - Ymh_{i,jj,j} \cdot \Gamma \le 0 \quad (j \ne jj) \quad \forall i,j,jj \tag{39}$$

$$Ymh_{i,j,jj} + Ymh_{i,jj,j} \le 1 \quad \forall i,j,jj \tag{40}$$

$$\sum_{k,kk} fc_{k,kk}^{j,i,ii} - Ymc_{j,i,ii} \cdot \Gamma \le 0 \quad (i \ne ii) \quad \forall i,ii,j \tag{41}$$

$$\sum_{k,kk} fc_{k,kk}^{j,ii,i} - Ymc_{j,ii,i} \cdot \Gamma \le 0 \quad (i \ne ii) \quad \forall i,ii,j \tag{42}$$

$$Ymc_{j,i,ii} + Ymc_{j,ii,i} \le 1 \quad \forall i,ii,j \tag{43}$$

where $Ymh_{i,j,jj}$ denotes the existence of the stream between heat exchanger matches (i,j) and (i,jj) and $Ymc_{j,i,ii}$ denotes the existence of the stream between heat exchanger matches (i,j) and (ii,j). The value of Γ is equal to F_i.

- *Area calculations*

The area of each exchanger can be expressed in terms of the heat loads and the temperature differences using Chen's (1987) approximation for the logarithmic mean temperature differences:

$$Q_{i,j,k} - A_{i,j,k} U_{i,j,k} \sqrt[3]{\Delta Th_{i,j,k} \Delta Tc_{i,j,k} \frac{\left[\Delta Th_{i,j,k} + \Delta Tc_{i,j,k}\right]}{2}} = 0 \quad \forall i,j,k \tag{44}$$

$$Q_i^{CU} - A_i^{CU} U_i^{CU} \sqrt[3]{\Delta T_i^{CU} \left(T_i^{HOUT} - T_{IN,CU}\right) \frac{\left[\Delta T_i^{CU} + \left(T_i^{HOUT} - T_{IN,CU}\right)\right]}{2}} = 0 \quad \forall i \tag{45}$$

$$Q_j^{HU} - A_j^{HU} U_j^{HU} \sqrt[3]{\Delta T_j^{HU} \left(T_{IN,HU} - T_j^{COUT}\right) \frac{\left[\Delta T_j^{HU} + \left(T_{IN,HU} - T_j^{COUT}\right)\right]}{2}} = 0 \quad \forall j \tag{46}$$

- *Maximum temperature differences for mixers*

When mixing streams that have different temperatures, there is a concern about mechanical stresses in mixers. Thus, in order to limit the temperature differences between streams that mix, we use the following constraint:

$$\alpha_{i,j,k} - \beta_{i,j,k} \le TMMax_{i,j,k} \quad \forall i,j,k \tag{47}$$

where $\alpha_{i,j,k}$ is the highest temperature of all the streams entering the mixer and $\beta_{i,j,k}$, is the lowest temperature of all streams that are mixing. $TMMax_{i,j,k}$ is the maximum difference of temperatures allowed in a mixer. To identify $\alpha_{i,j,k}$ and $\beta_{i,j,k}$, we introduce new binary variables $Rh_{l1}^{i,j,k}$ and $rh_{k,kk}^{i,j,jj}$ to denote the existence of streams with non-zero flow entering the mixer. If $Rh_{l1}^{i,j,k}$ is one when $Fh_{l1}^{i,j,k}$ has nonzero flow and zero otherwise. If $rh_{k,kk}^{i,j,jj}$ is one when $fh_{k,kk}^{i,j,jj}$ has nonzero flow and zero otherwise.

$$Fh_{l1}^{i,j,k} - \Gamma \cdot Rh_{l1}^{i,j,k} \le 0 \quad \forall i,j,k \tag{48}$$

$$fh_{k,kk}^{i,j,jj} - \Gamma \cdot rh_{k,kk}^{i,j,jj} \le 0 \quad \forall i,j,jj,k,kk \tag{49}$$

With these, we now determine the maximum and minimum temperatures among all mixing streams.

- *Maximum temperature among all hot streams in mixers*

$$\alpha_{i,j,k} \ge Th_{in}^{i,j,k} - \Gamma \cdot \left(1 - Rh_{in}^{i,j,k}\right) \quad \forall i,j,k \tag{50}$$

$$\alpha_{i,j,k} \le Th_{in}^{i,j,k} + \Gamma \cdot \left(1 - Rh_{in}^{i,j,k}\right) + M \cdot \left(1 - PHup_{in}^{i,j,k}\right) \quad \forall i,j,k \tag{51}$$

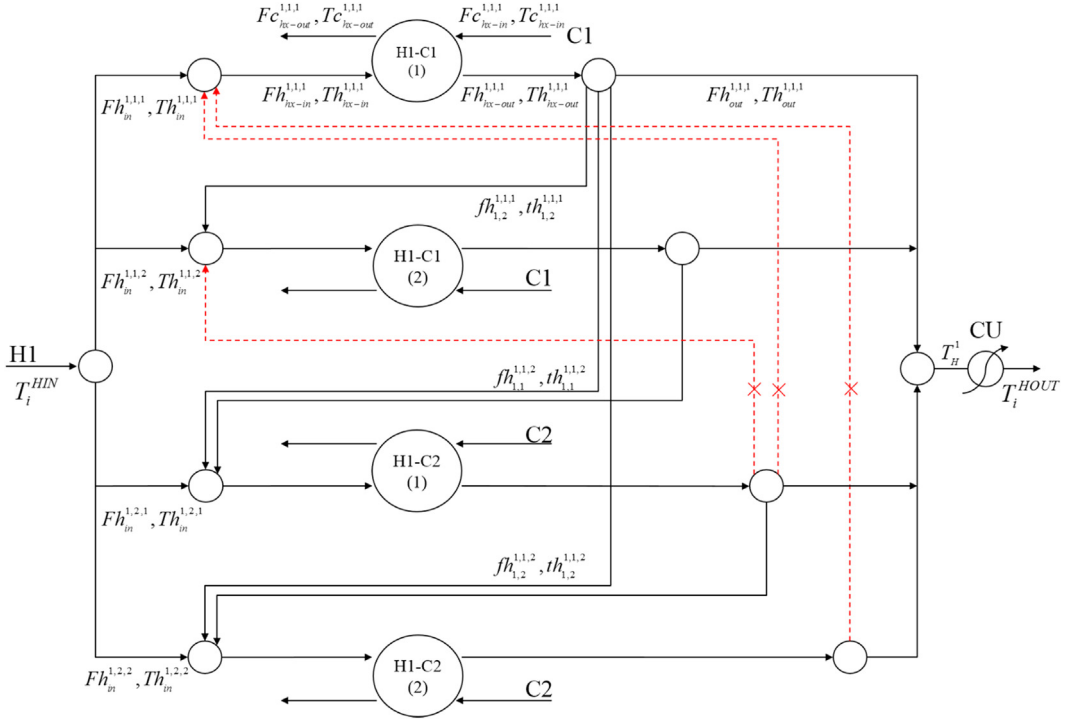

Fig. 3. Forbidden recycles.

$$\alpha_{i,j,k} \geq th^{i,jj,j}_{kk,k} - \Gamma \cdot \left(1 - rh^{i,jj,j}_{kk,k}\right) \quad \forall i,j,jj,k,kk \tag{52}$$

$$\alpha_{i,j,k} \leq th^{i,jj,j}_{kk,k} + \Gamma \cdot \left(1 - rh^{i,jj,j}_{kk,k}\right) + M \cdot \left(1 - pHup^{i,jj,j}_{kk,k}\right) \quad \forall i,j,jj,k,kk \tag{53}$$

where $PHup^{i,j,k}_{in}$ and $pHup^{i,jj,j}_{kk,k}$ are binary variables to denote that $Th^{i,j,k}_{in}$or $th^{i,jj,j}_{kk,k}$ are the highest values. Thus, for consistency, we request that

$$PHup^{i,j,k}_{in} + \sum_{jj,kk} pHup^{i,jj,j}_{kk,k} = Z_{i,j,k} \quad \forall i,j,k \tag{54}$$

$$PHup^{i,j,k}_{in} \leq Rh^{i,j,k}_{in} \quad \forall i,j,k \tag{55}$$

$$pHup^{i,j,jj}_{k,kk} \leq rh^{i,j,jj}_{k,kk} \quad \forall i,j,jj,k,kk \tag{56}$$

- *Minimum temperature among all hot streams in mixers*

$$\beta_{i,j,k} \leq Th^{i,j,k}_{in} + \Gamma \cdot \left(1 - Rh^{i,j,k}_{in}\right) \quad \forall i,j,k \tag{57}$$

$$\beta_{i,j,k} \geq Th^{i,j,k}_{in} - \Gamma \cdot \left(1 - Rh^{i,j,k}_{in}\right) - M \cdot \left(1 - PHlo^{i,j,k}_{in}\right) \quad \forall i,j,k \tag{58}$$

$$\beta_{i,j,k} \leq th^{i,jj,j}_{kk,k} + \Gamma \cdot \left(1 - rh^{i,jj,j}_{kk,k}\right) \quad \forall i,j,jj,k,kk \tag{59}$$

$$\beta_{i,j,k} \geq th^{i,jj,j}_{kk,k} - \Gamma \cdot \left(1 - rh^{i,jj,j}_{kk,k}\right) - M \cdot \left(1 - pHlo^{i,jj,j}_{kk,k}\right) \quad \forall i,j,jj,k,kk \tag{60}$$

where $PHlo^{i,j,k}_{in}$ and $pHlo^{i,jj,j}_{kk,k}$ are binary variables to denote that $Th^{i,j,k}_{in}$or $th^{i,jj,j}_{kk,k}$ are the lowest value.

$$PHlo^{i,j,k}_{in} + \sum_{jj,kk} pHlo^{i,jj,j}_{kk,k} = Z_{i,j,k} \quad \forall i,j,k \tag{61}$$

$$PHlo^{i,j,k}_{in} \leq Rh^{i,j,k}_{in} \quad \forall i,j,k \tag{62}$$

$$pHlo^{i,j,jj}_{k,kk} \leq rh^{i,j,jj}_{k,kk} \quad \forall i,j,k \tag{63}$$

An analogous procedure is applied to limit maximum and minimum temperatures of cold streams inlet to mixers.

2.1. Number of branches upon splitting

We consider limiting the number of streams in which each stream can divide. Consider $NSplit_i$ to be the maximum number of splits one stream can divide. Then we write:

$$\sum_{j,k} Rh^{i,j,k}_{in} \leq NSplit_i \quad \forall i \tag{64}$$

$$Rh^{i,j,k}_{out} + \sum_{jj,kk} rh^{i,j,jj}_{k,kk} \leq NSplit_i \quad \forall i,j,k \tag{65}$$

2.2. Number of splits

We also limit the number of times a stream is split as means to search simpler networks. This is accomplished by the following constraints

$$\left(\sum_{j,k} Rh^{i,j,k}_{in} - 1\right) - Sh_i \cdot \Gamma \leq 0 \quad \forall i \tag{66}$$

$$\left(Rh^{i,j,k}_{out} + \sum_{jj,kk} rh^{i,j,jj}_{k,kk} - 1\right) - Shh_{i,j,k} \cdot \Gamma \leq 0 \quad \forall i,j,k \tag{67}$$

where Sh_i and $Shh_{i,j,k}$ are binary variables indicating that there is a split. Thus, we write:

$$Sh_i + \sum_{j,k} Shh_{i,j,k} \leq TSplit_i \quad \forall i \tag{68}$$

that is, limiting the number of times stream i splits to be smaller than $TSplit_i$. Similar equations are written for cold streams.

- *Objective Function*

The objective we use is total annualized cost.

$$\begin{aligned} \min & \sum_i Q^{CU}_i \cdot CUcost + \sum_j Q^{HU}_j \cdot HUcost \\ & + C_{fixed}\left(\sum_{i,j,k} Z_{i,j,k} + \sum_i Z^{CU}_i + \sum_j Z^{HU}_j\right)/n \\ & + \left(C_{i,j,k}\sum_{i,j,k} A_{i,j,k} + C_i \sum_i A^{CU}_i + C_j \sum_j A^{HU}_j\right)/n \end{aligned} \tag{69}$$

3. Reformulation

We introduce the following new variables $\left(FTh^{i,j,k}_{l1}, fth^{i,j,jj}_{k,kk}, FTc^{i,j,k}_{l2}, ftc^{j,i,ii}_{k,kk}\right)$ to decompose the bilinear functions in the heat balance equations in the heat exchangers and mixers. These new variables will play a role later when using RYSIA.

$$Fh^{i,j,k}_{l1} \times Th^{i,j,k}_{l1} = FTh^{i,j,k}_{l1} \quad \forall i,j,k,l1 \tag{70}$$

$$fh^{i,j,jj}_{k,kk} \times th^{i,j,jj}_{k,kk} = fth^{i,j,jj}_{k,kk} \quad \forall i,j,jj,k,kk \tag{71}$$

$$Fc^{i,j,k}_{l2} \times Tc^{i,j,k}_{l2} = FTc^{i,j,k}_{l2} \quad \forall i,j,k,l2 \tag{72}$$

$$fc^{j,i,ii}_{k,kk} \times tc^{j,i,ii}_{k,kk} = ftc^{j,i,ii}_{k,kk} \quad \forall i,ii,j,k,kk \tag{73}$$

Then the heat balance Eqs. (7)–(12) are changed to the linear equations like below:

$$F_i T^i_H - \sum_j \sum_k FTh^{i,j,k}_{out} = 0 \quad \forall i \tag{74}$$

$$F_j T^j_C - \sum_i \sum_k FTc^{i,j,k}_{out} = 0 \quad \forall j \tag{75}$$

$$FTh^{i,j,k}_{in} + \sum_{jj} \sum_{kk} fth^{i,jj,j}_{kk,k} - FTh^{i,j,k}_{hx-in} = 0 \quad (k \geq kk) \quad \forall i,j,k \tag{76}$$

$$FTc^{i,j,k}_{in} + \sum_{ii} \sum_{kk} ftc^{j,ii,i}_{kk,k} - FTc^{i,j,k}_{hx-in} = 0 \quad (k \geq kk) \quad \forall i,j,k \tag{77}$$

$$Q_{i,j,k} - \left(FTh^{i,j,k}_{hx-in} - FTh^{i,j,k}_{hx-out}\right) = 0 \quad \forall i,j,k \tag{78}$$

$$Q_{i,j,k} - \left(FTc^{i,j,k}_{hx-in} - FTc^{i,j,k}_{hx-out}\right) = 0 \quad \forall i,j,k \tag{79}$$

4. Full bilinear model reformulation

The lower bound model can be made bilinear as follows: We start with Eq. (44) and we propose the following set of transformations:

$$\frac{Q_{i,j,k}}{U_{i,j,k}} - A_{i,j,k}\sqrt[3]{\Delta Th_{i,j,k}\Delta Tc_{i,j,k}\frac{(\Delta Th_{i,j,k} + \Delta Tc_{i,j,k})}{2}} = 0$$

$$\Leftrightarrow \begin{cases} \frac{Q_{i,j,k}}{U_{i,j,k}} - A_{i,j,k} \cdot DT_{i,j,k} = 0 \\ DT^3_{i,j,k} = \Delta \mathrm{Th}_{\mathrm{i,j,k}} \Delta Tc_{i,j,k} \frac{(\Delta Th_{i,j,k} + \Delta Tc_{i,j,k})}{2} \end{cases} \tag{80}$$

$$\begin{cases} \frac{Q_{i,j,k}}{U_{i,j,k}} - A_{i,j,k} \cdot DT_{i,j,k} = 0 \\ DT^3_{i,j,k} = \frac{\left(\Delta Th^2_{i,j,k} \Delta Tc_{i,j,k} + \Delta Tc^2_{i,j,k} \Delta Th_{i,j,k}\right)}{2} \end{cases}$$

$$\Leftrightarrow \begin{cases} \frac{Q_{i,j,k}}{U_{i,j,k}} - A_{i,j,k} \cdot DT_{i,j,k} = 0 \\ WDT_{i,j,k} = DT^2_{i,j,k} DT_{i,j,k} \\ WDT_{i,j,k} = \frac{\left(\Delta Th^2_{i,j,k} \Delta Tc_{i,j,k} + \Delta Tc^2_{i,j,k} \Delta Th_{i,j,k}\right)}{2} \end{cases} \tag{81}$$

$$\begin{cases} \frac{Q_{i,j,k}}{U_{i,j,k}} - A_{i,j,k} \cdot DT_{i,j,k} = 0 \\ WDT_{i,j,k} = DT^2_{i,j,k} DT_{i,j,k} \\ WDT_{i,j,k} = \frac{\left(\Delta Th^2_{i,j,k} \Delta Tc_{i,j,k} + \Delta Tc^2_{i,j,k} \Delta Th_{i,j,k}\right)}{2} \end{cases} \Leftrightarrow \begin{cases} \frac{Q_{i,j,k}}{U_{i,j,k}} - A_{i,j,k} \cdot DT_{i,j,k} = 0 \\ WDT_{i,j,k} = YDT_{i,j,k} DT_{i,j,k} \\ YDT_{i,j,k} = DT^2_{i,j,k} \\ WDT_{i,j,k} = S_{i,j,k} + R_{i,j,k} \\ 2S_{i,j,k} = \Delta Th^2_{i,j,k} \Delta Tc_{i,j,k} \\ 2R_{i,j,k} = \Delta Tc^2_{i,j,k} \Delta Th_{i,j,k} \end{cases} \tag{82}$$

$$\begin{cases} \frac{Q_{i,j,k}}{U_{i,j,k}} - A_{i,j,k} \cdot DT_{i,j,k} = 0 \\ WDT_{i,j,k} = YDT_{i,j,k} DT_{i,j,k} \\ YDT_{i,j,k} = DT^2_{i,j,k} \\ WDT_{i,j,k} = S_{i,j,k} + R_{i,j,k} \\ 2S_{i,j,k} = \Delta Th^2_{i,j,k} \Delta Tc_{i,j,k} \\ 2R_{i,j,k} = \Delta Tc^2_{i,j,k} \Delta Th_{i,j,k} \end{cases} \Leftrightarrow \begin{cases} \frac{Q_{i,j,k}}{U_{i,j,k}} - A_{i,j,k} \cdot DT_{i,j,k} = 0 \\ WDT_{i,j,k} = YDT_{i,j,k} DT_{i,j,k} \\ YDT_{i,j,k} = DT^2_{i,j,k} \\ WDT_{i,j,k} = S_{i,j,k} + R_{i,j,k} \\ 2S_{i,j,k} = MT_{i,j,k} \Delta Tc_{i,j,k} \\ 2R_{i,j,k} = NT_{i,j,k} \Delta Th_{i,j,k} \\ MT_{i,j,k} = \Delta Th^2_{i,j,k} \\ NT_{i,j,k} = \Delta Tc^2_{i,j,k} \end{cases} \tag{83}$$

The same can be written for Eqs. (45) and (46). For this bilinear model, one can use the same strategy for relaxation to obtain a lower bound model as presented by Faria et al. (2011, 2015).

5. Lower bound model

In the bilinear terms, we choose temperature to be the partitioned variable. In turn, the area equations are treated using the image-partitioning model (Faria et al., 2015).

5.1. Bilinear terms

Eqs. (70)–(73) are considered for this decomposition.

- **Partitioning** $Th^{i,j,k}_{l1}$

$$\sum_o ThD^{i,j,k,o}_{l1} \times vThD^{i,j,k,o}_{l1} \le Th^{i,j,k}_{l1} \le \sum_o ThD^{i,j,k,o+1}_{l1} \times vThD^{i,j,k,o}_{l1} \quad \forall i,j,k,l1 \tag{84}$$

$$\sum_o vThD^{i,j,k,o}_{l1} = 1 \quad \forall i,j,k,l1 \tag{85}$$

We partition flowrate $Th^{i,j,k}_{l1}$ using o intervals. Then $FTh^{i,j,k}_{l1}$ is bounded by the following relations.

$$FTh^{i,j,k}_{l1} \ge \sum_o ThD^{i,j,k,o}_{l1} \times FhB^{i,j,k,o}_{l1} \quad \forall i,j,k,l1 \tag{86}$$

$$FTh^{i,j,k}_{l1} \le \sum_o ThD^{i,j,k,o+1}_{l1} \times FhB^{i,j,k,o}_{l1} \quad \forall i,j,k,l1 \tag{87}$$

The variable $FhB^{i,j,k,o}_{l1}$ is introduced to replace the product of the partitioned flowrates and binary variables. According to the direct partitioning procedures (DPP1) of (Faria and Bagajewicz, 2011b), we have.

$$FhB^{i,j,k,o}_{l1} \ge 0 \quad \forall i,j,k,l1,o \tag{88}$$

$$FhB^{i,j,k,o}_{l1} - F_i \times vThD^{i,j,k,o}_{l1} \le 0 \quad \forall i,j,k,l1,o \tag{89}$$

$$\left(Fh^{i,j,k}_{l1} - FhB^{i,j,k,o}_{l1}\right) - F_i \times \left(1 - vThD^{i,j,k,o}_{l1}\right) \le 0 \quad \forall i,j,k,l1,o \tag{90}$$

$$Fh^{i,j,k}_{l1} - FhB^{i,j,k,o}_{l1} \ge 0 \quad \forall i,j,k,l1,o \tag{91}$$

The same procedure is used to partition $Tc^{i,j,k}_{l2}$, $th^{i,j,jj}_{k,kk}$ and $tc^{j,i,ii}_{k,kk}$.

5.2. Nonlinear function

We now work on Eq. (44), by partitioning the temperature differences first, as follows:

$$\sum_{n1} \Delta ThD_{i,j,k,n1} \times Yh_{i,j,k,n1} \le \Delta Th_{i,j,k} \le \sum_{n1} \Delta ThD_{i,j,k,n1+1} \times Yh_{i,j,k,n1} \quad \forall i,j,k \tag{92}$$

$$\sum_{n2} \Delta TcD_{i,j,k,n2} \times Yc_{i,j,k,n2} \le \Delta Tc_{i,j,k} \le \sum_{n2} \Delta TcD_{i,j,k,n2+1} \times Yc_{i,j,k,n2} \quad \forall i,j,k \tag{93}$$

Thus, Eqs. (20) and (21) can be rewritten as follows:

$$Th^{i,j,k}_{hx-in} - Tc^{i,j,k}_{hx-out} \le \sum_{n1} \Delta ThD_{i,j,k,n1+1} Yh_{i,j,k,n1} + \Gamma(1 - Z_{i,j,k}) \quad \forall i,j,k \tag{94}$$

$$Th^{i,j,k}_{hx-in} - Tc^{i,j,k}_{hx-out} \ge \sum_{n1} \Delta ThD_{i,j,k,n1} Yh_{i,j,k,n1} - \Gamma(1 - Z_{i,j,k}) \quad \forall i,j,k \tag{95}$$

$$Th^{i,j,k}_{hx-out} - Tc^{i,j,k}_{hx-in} \le \sum_{n2} \Delta TcD_{i,j,k,n2+1} Yc_{i,j,k,n2} + \Gamma(1 - Z_{i,j,k}) \quad \forall i,j,k \tag{96}$$

$$Th^{i,j,k}_{hx-out} - Tc^{i,j,k}_{hx-in} \ge \sum_{n2} \Delta TcD_{i,j,k,n2} Yc_{i,j,k,n2} - \Gamma(1 - Z_{i,j,k}) \quad \forall i,j,k \tag{97}$$

$$\sum_{n1} Yh_{i,j,k,n1} = Z_{i,j,k} \quad \forall i,j,k \tag{98}$$

$$\sum_{n2} Yc_{i,j,k,n2} = Z_{i,j,k} \quad \forall i,j,k \tag{99}$$

Now we rewrite Eq. (44) as follows:

$$\frac{Q_{i,j,k}}{U_{i,j,k}} - A_{i,j,k} \sum_{n1} \sum_{n2} Yh_{i,j,k,n1} Yc_{i,j,k,n2} \sqrt[3]{\Delta ThD_{i,j,k,n1+1} \Delta TcD_{i,j,k,n2+1} \frac{(\Delta ThD_{i,j,k,n1+1} + \Delta TcD_{i,j,k,n2+1})}{2}} \le 0 \quad \forall i,j,k \tag{100}$$

Next, after substituting the product of binaries ($Yh_{i,j,k,n1}$, $Yc_{i,j,k,n2}$) and area ($A_{i,j,k}$) in Eq. (100) with new positive continuous variable($H_{i,j,k,n1,n2}$), we get:

$$\frac{Q_{i,j,k}}{U_{i,j,k}} - \sum_{n1} \sum_{n2} H_{i,j,k,n1,n2} \sqrt[3]{\Delta ThD_{i,j,k,n1+1} \Delta TcD_{i,j,k,n2+1} \frac{(\Delta ThD_{i,j,k,n1+1} + \Delta TcD_{i,j,k,n2+1})}{2}} \le 0 \quad \forall i,j,k \tag{101}$$

To complement the above substitution, the following constraints are added:

$$\sum_{n1} H_{i,j,k,n1,n2} - \Omega Yc_{i,j,k,n2} \le 0 \quad \forall i,j,k,n2 \tag{102}$$

$$\sum_{n2} H_{i,j,k,n1,n2} - \Omega Yh_{i,j,k,n1} \le 0 \quad \forall i,j,k,n1 \tag{103}$$

$$\sum_{n1}\sum_{n2} H_{i,j,k,n1,n2} = A_{i,j,k} \quad \forall i,j,k \tag{104}$$

A similar procedure can be applied to Eqs. (45) and (46). Finally, in the case of the fully bilinear model we need to partition $DT_{i,j,k}$, $\Delta Th_{i,j,k}$ and $\Delta Tc_{i,j,k}$:

$$\left\{ \sum_l \hat{D}_{i,j,k,l}\, r_{i,j,k,l} \le DT_{i,j,k} \le \sum_l \hat{D}_{i,j,k,l+1} r_{i,j,k,l} \sum_l r_{i,j,k,l} = 1 \right. \tag{105}$$

where $\hat{D}_{i,j,k,l}$ are given by all possible values of the cubic root equation. The partitioning of $\Delta Th_{i,j,k}$ and $\Delta Tc_{i,j,k}$ are already considered above.

6. Lifting partitioning

To help increasing (to lift) the lower bound value, we resort to partitioning of variables that participate in the objective function. For these we introduce new variables for the total utility usage and the total area.

$$\sum_j Q_j^{HU} = TQ \tag{106}$$

$$\sum_{i,j,k} A_{i,j,k} = TA \tag{107}$$

These new variables TA and TQ are partitioned using m and p intervals. We use binary variables vTQ_m for TQ and vTA_p for TA.

$$\sum_m (TQD_m \cdot vTQ_m) \le TQ \le \sum_m (TQD_{m+1} \cdot vTQ_m) \tag{108}$$

$$\sum_m vTQ_m = 1 \tag{109}$$

$$\sum_p (TAD_p \cdot vTA_p) \le TA \le \sum_p (TAD_{p+1} \cdot vTA_p) \tag{110}$$

$$\sum_p vTA_p = 1 \tag{111}$$

TQD_m and TAD_p are discrete points of the total area and exchanged heat of heater.

We also experimented with partitioning of variables representing the product of flow and temperature, in Eqs. (70)–(74), namely $FTh_{l1}^{i,j,k}, FTc_{l2}^{i,j,k}, fth_{k,kk}^{i,j,jj}$ and $ftc_{k,kk}^{i,j,jj}$. We introduce new binary variables $vFTh_{l1}^{i,j,k}, vFTc_{l2}^{i,j,k}, vfth_{k,kk}^{i,j,jj}$ and $vftc_{k,kk}^{i,j,jj}$ for this purpose.

$$\sum_o \left(dFTh_{l1}^{i,j,k,o} \cdot vFTh_{l1}^{i,j,k,o} \right) \le FTh_{l1}^{i,j,k} \le \sum_o \left(dFTh_{l1}^{i,j,k,o+1} \cdot vFTh_{l1}^{i,j,k,o} \right) \tag{112}$$

$$\sum_o vFTh_{l1}^{i,j,k} = 1 \tag{113}$$

$$\sum_o \left(dFTc_{l2}^{i,j,k,o} \cdot vFTc_{l2}^{i,j,k,o} \right) \le FTc_{l2}^{i,j,k} \le \sum_o \left(dFTc_{l2}^{i,j,k,o+1} \cdot vFTc_{l2}^{i,j,k,o} \right) \tag{114}$$

$$\sum_o vFTc_{l2}^{i,j,k} = 1 \tag{115}$$

$$\sum_o \left(dfth_{k,kk}^{i,j,jj,o} \cdot vfth_{k,kk}^{i,j,jj,o} \right) \le fth_{k,kk}^{i,j,jj} \le \sum_o \left(dfth_{k,kk}^{i,j,jj,o+1} \cdot vfth_{k,kk}^{i,j,jj,o} \right) \tag{116}$$

$$\sum_o vfth_{k,kk}^{i,j,jj,o} = 1 \tag{117}$$

$$\sum_o \left(dftc_{k,kk}^{j,i,ii,o} \cdot vftc_{k,kk}^{j,i,ii,o} \right) \le ftc_{k,kk}^{j,i,ii} \le \sum_o \left(dftc_{k,kk}^{j,i,ii,o+1} \cdot vftc_{k,kk}^{j,i,ii,o} \right) \tag{118}$$

$$\sum_o vftc_{k,kk}^{j,i,ii,o} = 1 \tag{119}$$

$dFTh_{l1}^{i,j,k}, dFTc_{l2}^{i,j,k}, dfth_{k,kk}^{i,j,jj}$ and $dftc_{k,kk}^{i,j,jj}$ are discrete points of the bilinear variables.

7. RYSIA's solution strategy

After partitioning each one of the variables in the bilinear terms and the nonconvex terms, our method consists of a bound contraction step that uses a procedure for eliminating intervals. In the heat exchanger network problems the bilinear terms are composed of the product of heat capacity flow rates and stream temperatures, and the nonconvex terms are the logarithmic mean temperature differences of the area calculation. The partitioning methodology generates linear models that guarantee to be lower bounds of the problems. upper bounds are needed for the bound contraction procedure. These upper bounds are usually obtained using the original MINLP model often initialized by the results from the lower bound model.

We defined different variables:

- partitioning variables, which are the ones that generate several intervals and are used to construct linear relaxations of bilinear and nonconvex terms,
- bound contracted variables, which are also partitioned into intervals, but only for the purpose of performing their bound contraction (these are those that participate in the lifting), and
- branch and bound variables, which are the variables for which a branch and bound procedure is tried (they need not be the same set as the other two types of variables).

The global optimization strategy is now summarized as follows: we run the lower bound model first. Then we use the result of the lower bound model as initial values for the upper bound model. If the upper bound model turns infeasible, we fix all integers $Z_{i,j,k}, Rh_{l1}^{i,j,k}, Rc_{l2}^{i,j,k}, rhh_{k,kk}^{i,j,jj}$ and $rcc_{k,kk}^{j,i,ii}$ to be the same as those provided by the lower bound, we ignore the mixing constraints and solve the resulting NLP problem. If, in turn this NLP fails, we additionally fix the $Q_{i,j,k}$ values to be the given by the lower bound and solve again as an NLP. Finally, if these last also fails to give a feasible solution, we fix all flows and remove the area equations and area cost from the objective and solve the resulting LP problem. The area can be calculated from the LP solution and therefore the cost of a feasible point is obtained. After the upper bound is computed, we proceed to perform bound contraction on all variables as explained below.

7.1. RYSIA's bound contraction method

The bound contraction procedure used in the interval elimination strategy used by RYSIA and presented by Faria and Bagajewicz (2011b, 2011c) and Faria et al (2015). We summarized the basic strategy in this section. Further details of different strategies can be found in the original paper.

1. Run the lower bound model to calculate a lower bound (LB) of the problem and identify the intervals containing the solution of the lower bound model.
2. Run the original MINLP initialized by the solution of the lower bound model to find an upper bound (UB) solution. If there is failure use the alternatives provided above.
3. Calculate the gap between the upper bound solution and the lower bound solution. If the gap is lower than the tolerance, the solution was found. Otherwise go to the step 4.
4. Run the lower bound model

a) forbidding one of the intervals identified in step 1, or
b) forbidding all the intervals including the one identified in step 1, except the most distant.

5. Repeat step 4 for all the other variables, one at a time.
6. Go back to step 1 (a new iteration using contracted bounds starts).

In step 4) if the solution is infeasible or if it is feasible but larger than the upper bound, then all the intervals that have not been forbidden for this variable are eliminated. The surviving region between the new bounds is re-partitioned. If the solution is feasible but lower than the upper bound, we cannot bound contract and we move to the next variable.

The detailed illustration of the interval elimination using the bound contraction procedures was introduced in our previous publications using examples (Faria and Bagajewicz, 2011b, 2011c; Faria et al., 2015). In those papers, different options for bound contracting have been introduced: one-pass interval elimination, cyclic elimination, single and extended interval forbidding (Fig. 4), etc., all of which are detailed in the article referenced.

The process is repeated with new bounds until convergence or until the bounds cannot be contracted anymore. If the bound contraction does not occur anymore, we suggest increasing the number of intervals and starting over. An alternative is branch and bound but we already showed that is more time consuming, especially if we use bound contracting at each node (Faria et al., 2015).

7.2. RYSIA's upper bound calculation

We use the lower bound solution values as initial point for the upper bound MINLP. However, when such MINLP fails (we used DICOPT), we fix all integers $Z_{i,j,k}$, $Rh_{l1}^{i,j,k}$, $Rc_{l2}^{i,j,k}$, $rhh_{k,kk}^{i,j,jj}$ and $rcc_{k,kk}^{j,i,ii}$ to be the same as those provided by the lower bound, and solve the resulting NLP problem. If, in turn this NLP fails, we additionally fix the $Q_{i,j,k}$ values to be the given by the lower bound and solve again as an NLP. Finally, if these last also fails to give a feasible solution, we fix all flows and remove the area equations and area cost from the objective and solve the resulting LP problem. The area can be calculated from the LP solution and therefore the cost of a feasible point is obtained. We did not experiment with alternatives to this sequence.

We also found that in the above process the upper bound is trapped in a point that is not optimal. We obtain solutions containing bypasses around exchangers like the ones shown in Fig. 5.

To address this anomaly, there are two strategies. One is to tolerate the anomaly until the end and remove them then. This is legitimate because the upper bound does not have to be any local optimum. It could be any good feasible point.

However, if one wants to prevent the model from having such bypasses, then the following constraints can be added to the upper bound model.

$$\sum_{jj,kk} rh_{kk,k}^{i,jj,j} \le NSplit_i \cdot ih_{i,j,k} \quad \forall i,j,k \tag{120}$$

$$\sum_{ii,kk} rc_{kk,k}^{j,ii,i} \le NSplit_j \cdot ic_{i,j,k} \quad \forall i,j,k \tag{121}$$

$$\sum_{jj,kk} rh_{k,kk}^{i,j,jj} \le NSplit_i \cdot bh_{i,j,k} \quad \forall i,j,k \tag{122}$$

$$\sum_{ii,kk} rc_{k,kk}^{j,i,ii} \le NSplit_j \cdot bc_{i,j,k} \quad \forall i,j,k \tag{123}$$

$$Rh_{in}^{i,j,k} + ih_{i,j,k} \le 1 \quad \forall i,j,k \tag{124}$$

$$Rc_{in}^{i,j,k} + ic_{i,j,k} \le 1 \quad \forall i,j,k \tag{125}$$

$$Rh_{out}^{i,j,k} + bh_{i,j,k} \le 1 \quad \forall i,j,k \tag{126}$$

$$Rc_{out}^{i,j,k} + bc_{i,j,k} \le 1 \quad \forall i,j,k \tag{127}$$

$$rh_{k,kk}^{i,jj,jjj} \le 2 - rh_{k,kk}^{i,j,jj} - rh_{k,kk}^{i,j,jjj} \quad \forall i,j,jj,jjj,k,kk \tag{128}$$

$$rc_{k,kk}^{j,ii,iii} \le 2 - rc_{k,kk}^{j,i,ii} - rc_{k,kk}^{j,i,iii} \quad \forall j,i,ii,iii,k,kk \tag{129}$$

where $ih_{i,j,k}$ and $ic_{i,j,k}$ denote the existence of inlet streams from other exchangers. In addition, $bh_{i,j,k}$ and $bc_{i,j,k}$ denote the existence of outlet streams going to other exchangers.

8. Examples

Three examples of different sizes are presented. The examples were implemented in GAMS (version 23.7) (Brooke et al., 2007) and solved using CPLEX (version 12.3) as the MIP solver and DICOPT (Viswanathan and Grossmann, 1990) as the MINLP solver on a PC machine (Xeon 3.2 GHz, 8GB RAM).

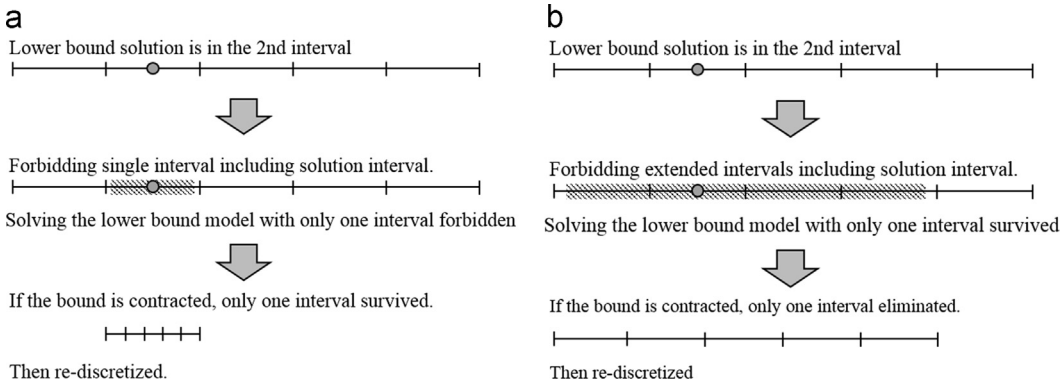

Fig. 4. (a) Single interval forbidding, (b) Extended intervals forbidding.

Example 1: The first example is 10SP1 (Cerda, 1980). This example consists of four hot and five cold streams and the data is given in Tables 1 and 2. This example was solved using a superstructure including one exchanger per match ($k=1$) and we first did not limit the number of splits, as well as the number of splitting. We assumed a minimum temperature approach $EMAT_{i,j}$ of 10 °C and there is no double recycling stream in the network.

We partitioned Delta T and stream temperature with 2 intervals and used the lifting partitioning and the extended interval forbidding. Lower limits of total area and total heat of heating utilities in the lifting partitioning are used for 3000 m^2 and 150 KJ/s from (Faria et al., 2015). Upper limits are used 50% higher values than lower limits. We first run this problem without lifting partitioning. The disappointing results are shown in Table 3. We note that the number of intervals at the end is still 2, which means that in all iterations there was some bound contraction and that because there are 2 intervals, extended elimination resulted in single elimination.

The globally optimal solution features an annualized cost of $99,636,825 and was obtained in the root node of the 3th iteration satisfying 1% gap between UB and LB (see Table 4). The results are summarized in Table 5 and the optimal solution network is presented in Fig. 6. We run the branch and bound with lifting partitioning without bound contraction in each node (as in Faria et al., 2015). We obtained an objective value of $198,452,300 with 50% tolerance gap after 200 iterations using 43 min 10 s CPU time.

We also run the bilinear model with the lifting partitioning and obtained an objective value of $148,410,500 with 33% tolerance gap after 20 iterations using 59 min 37 s cup time. We need to also point out the price paid for considering alternatives to the stages model, which took 20 s or less to solve this problem in 5 iterations is fairly high, but tolerable for practical purposes. In addition, note that although we used extended elimination, there was no opportunity to employ it, as the number of intervals remains at 2. Finally, we note that even with such a small gap (1%) the solution is different than the one obtained by Faria et al. (2015), indicating that there are several alternative solutions close to the global optimum.

For comparison, we run BARON (Version 14.4) and after 2 h of computation, we obtained an upper bound value of 10^{50} and a lower bound of $5,615,430. ANTIGONE (Version 1.1), in turn, found an upper bound value of $99,650,000 with a 94% gap after 2 h running. We observe here the same behavior for ANTIGONE and RYSIA, that is, an early identification of the optimum and a subsequent improvement of the lower bound.

We added that the maximum temperature differences for mixers were lower than 30 °C (Eqs. (47)–(63)) to avoid high temperature difference in H4 and obtained an objective value of $ 99,618,825 with 0.88% tolerance gap using 2 h 00 min 2 s of cpu time. (Fig. 7). The structure of the HEN cannot be obtained with the stages model.

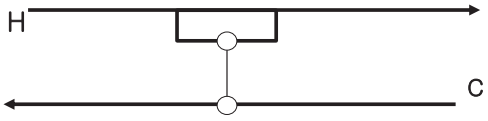

Fig. 5. Anomalies found in upper bound solutions.

Example 2: The third example consists of 11 hot and 2 cold streams corresponding to a crude fractionation unit. The data is given in Tables 6 and 7. We assumed a minimum temperature approach of $EMAT_{i,j}=10$ °C. We used a superstructure including one exchanger per match ($k=1$) and we first did not limit the temperatures upon mixing and the number of splits, as well as the number of splitting.

We partitioned Delta T and stream temperature with 2 intervals and used the lifting partitioning and the extended interval

Table 1
Data for example 1.

Stream	F [Kg/s]	Cp [kJ/Kg °C]	T_{in} [°C]	T_{out} [°C]	h [kJ/s m^2 °C]
H1	2.634	1	160	93	0.06
H2	3.162	1	249	138	0.06
H3	4.431	1	227	66	0.06
H4	5.319	1	199	66	0.06
C1	2.286	1	60	160	0.06
C2	1.824	1	116	222	0.06
C3	2.532	1	38	221	0.06
C4	5.184	1	82	177	0.06
C5	4.170	1	93	205	0.06
HU		1	38	82	0.06
CU		1	271	149	0.06

Table 2
Cost data for example 2.

Heating utility cost	566,167 [$/(kJ/s)]
Cooling utility cost	53,349 [$/(kJ/s)]
Fixed cost for heat exchangers	5291.9 [$/unit]
Variable cost for heat exchanger area	77.79 [$/$m^2$]

Table 4
Result of example 1 when using lifting partitioning.

# of interval	Objective value	Gap	# of bound contraction cycles	# of intervals at convergence	CPU time
2	$99,636,825	0.9%	3	2	22 m41 s

Table 5
Heat exchanger results for example 1.

	Area (m^2)	Duty [KJ/s]
EX1	190.20	130.73
EX2	328.63	228.60
EX3	672.48	336.31
EX4	716.08	316.00
EX5	264.86	309.03
EX6	248.37	176.48
EX7	130.28	150.82
EX8	2.17	3.51
EX9	83.94	41.95
CU1	219.87	115.84
CU2	263.94	139.01
HU	207.16	151.39
Total annual cost	$99,636,825	

Table 3
Results example 1 without lifting partitioning.

	# of starting intervals	Objective value (upper bound)	Lower bound	Gap	# of bound contraction cycles	# of intervals at convergence	CPU time
Extended elimination	**2**	$99,627,885	$5,620,271	94.4%	10	2	3 h 05 m

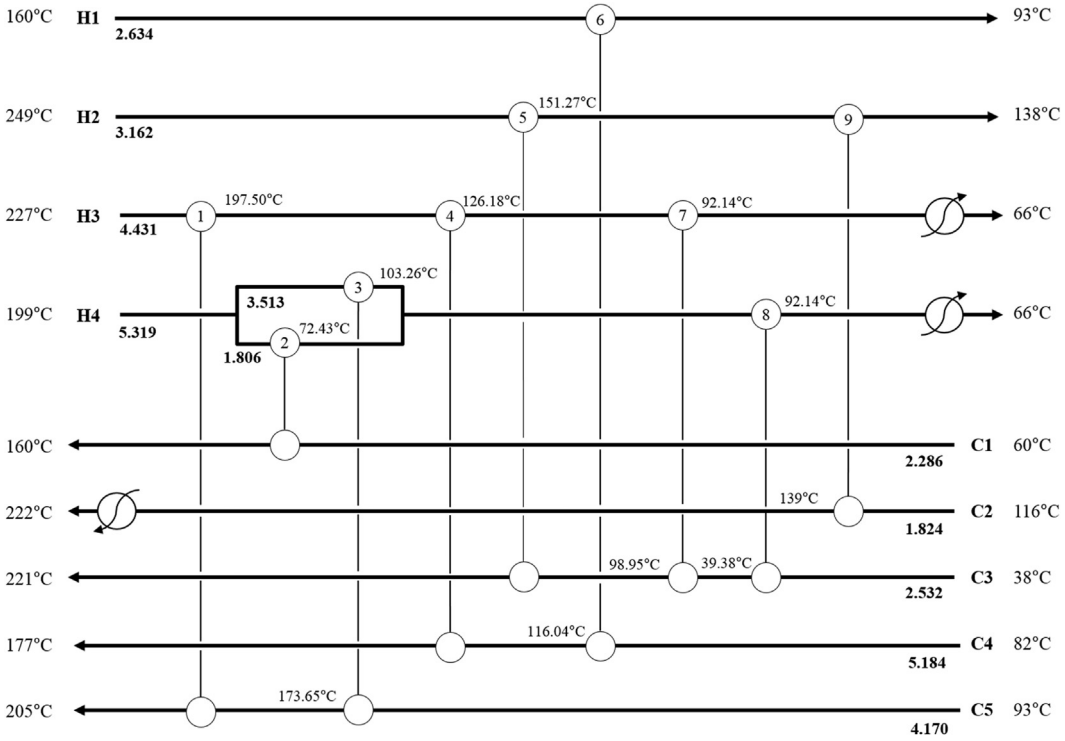

Fig. 6. The solution network for example 1.

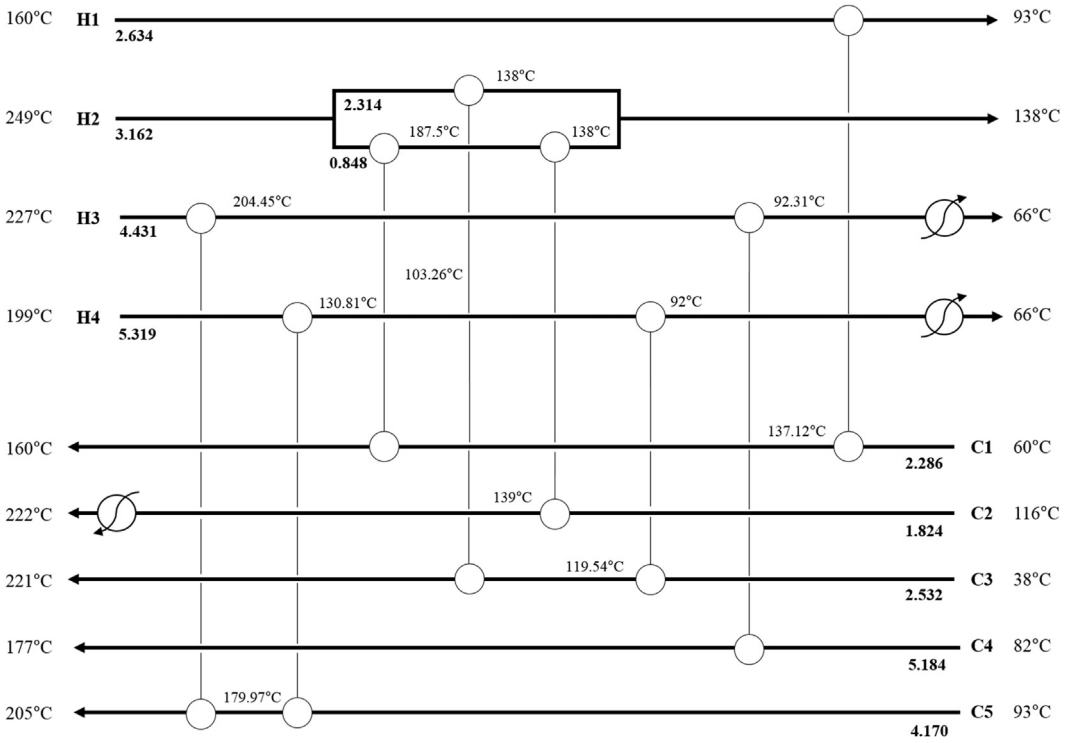

Fig. 7. The solution network for example 1 with mixing control (*TMMax* = 30 °C).

forbidding as in example 1. Lower limits of *TA* and *TQ* are 8636 m^2 and 23,566 KJ/s calculated from the pinch analysis. Upper limits are used 30% higher values than lower limits.

Without lifting partitioning, we obtained an objective value of $3,418,502 with 32.9% gap after 20 iterations employing 2 h 05 min 04 s of CPU time. We found the solution using lifting partitioning with a 1.8% gap between the UB and LB in Table 8. The results are summarized in Table 9. The optimum solution, presented in Fig. 8, has an annualized cost of $3,463,096. We tested using the branch and bound with the lifting partitioning without bound contraction in each node (as in Faria et al, 2015) and obtained an objective value of $3,486,497 with 3.9% tolerance gap after 200 iterations using 47 min 09 s CPU time. We also tested the bilinear model with the lifting partitioning and obtained an objective value of $3,513,866 with 4.7% tolerance gap after 40 iterations using 5 h 59 min 21 s cup time.

Table 6
Data for example 2.

Stream		FC_p [kJ/s C]	Cp [kJ/kg C]	T_{in} [C]	T_{out} [C]	H [kJ/s m^2 C]
H1	TCR	166.7	2.3	140.2	39.5	0.26
H2	LGO	45.8	2.5	248.8	110	0.72
H3	Kerosene	53.1	2.3	170.1	60	0.45
H4	HGO	35.4	2.5	277	121.9	0.57
H5	HVGO	198.3	2.4	250.6	90	0.26
H6	MCR	166.7	2.5	210	163	0.33
H7	LCR	291.7	2.9	303.6	270.2	0.41
H8	VR	84.3	1.7	360	241.4	0.47
H9	LVGO	68.9	2.5	178.6	108.9	0.6
H10	SR-quench	27.6	3.2	359.6	280	0.47
H11	VR2	84.3	1.7	241.4	280	0.47
C1	Crude	347.1	2.1	30	130	0.26
C2	Crude	347.9	3.0	130	350	0.72
HU			1	500	499	0.53
CU			1	20	40	0.53

Table 7
Cost data for example 2.

Heating utility cost	100 [$/(kJ/s)]
Cooling utility cost	10 [$/(kJ/s)]
Fixed cost for heat exchangers	250,000 [$/unit]
Variable cost for heat exchanger area	550 [$/m^2]

Table 8
Results of example 3 with the lifting partitioning and the extended interval forbidding.

# of interval	Objective value (upper bound)	Gap	# of bound contraction cycles	# of intervals at convergence	CPU time
2	3,463,096	1.8%	8	2	20 m 32 s

Table 9
Summary of results for example 3.

Total area	9793.84 m^2
Number of exchangers	17
Heating utility	23,566 kJ/s
Cooling utility	11783.5 kJ/s
Final objective function (Total annualized cost)	$3,463,096

In addition, we run BARON (Version 14.4) and after 2 h running, we obtained an upper bound value of $ 10^{50} and 2,317,170 for the lower bound. ANTIGONE (Version 1.1), in turn, found an upper bound value of $ 3,609,000 with a 36% gap after 2 h running. As in the other two examples, we see RYSIA and ANTIGONE, but not BARON, identifying solutions close to the global optimum early.

We also notice that VR1 is matching with the cold stream twice, but using branches of the same split. Structures like the ones shown in Fig. 8 also contain splits with more than one exchanger in each branch, something that models like the stages model (Yee and Grossmann, 1990) cannot capture. Moreover, the structure also contains splitting inside branches that the stages model cannot capture either. To avoid many splits in Fig. 9, the limitation on the number of splits (Eqs. ((64) and 65)) is used. The maximum number of splits limited to 3. We obtained an objective value of $3,483,611 with 2.4% tolerance gap after 15 iterations using 40 min 54 s cup time (Fig. 9).

Then, we added $Tsplit=1$ to avoid splitting two times and obtained an objective value of $3,502,522 with 2.9% tolerance gap after 6 iterations using 2 h 14 min 55 s cup time (Fig. 10).

Example 3: This last example is added to highlights some of the difficulties that one could encounter with certain problems. The example consists of three hot streams, two cold streams (Nguyen et al., 2010) (Tables 10 and 11). We assumed a minimum temperature approach $EMAT_{i,j}$ of 10 °C. We used a superstructure including two exchanger per match ($k=2$). The lower bounding MILP model has 853 binary variables, of which 494 are partitioning variables and 2096 continuous variables. We first run this model without any restrictions on the temperature difference in mixing (Eqs. (47)–(63)).

For the illustration of this example, we used two initial intervals of temperature differences ($\Delta Th_{i,j,k}$, $\Delta Tc_{i,j,k}$, ΔT_i^{CU}, ΔT_j^{HU}) and stream temperatures ($Th_{l1}^{i,j,k}$, $Tc_{l2}^{i,j,k}$, $th_{k,kk}^{i,j,jj}$, $tc_{k,kk}^{j,i,ii}$) for the lower bound model. When no interval was eliminated and the lower bound and upper bound gap was still larger than the tolerance, we increased the number of intervals.

We tried single and extended interval forbidding in the bound contraction procedure. In Table 12, we use partitioning of delta T and stream temperatures, without lifting partitioning and bilinear partitioning as described above. We note that if on additionally partition and bound contract area and Q values the time increases without any significant improvement.

We also run the branch and bound without bound contraction in each node (as in Faria et al, 2015) and obtained an objective value of $1,864,786 with 47% gap after 200 iterations employing 59 min 10 s of CPU time. For this, we partitioned ΔT and stream temperatures and performed the B&B on all partitioned variables. In addition, we run BARON (Version 14.4) and after 2 h running, we obtained an upper bound value of $2,895,060 with a 54% gap. ANTIGONE (Version 1.1), in turn, found an upper bound value of $ 1,767,000 with a 32% gap after 2 h running.

To improve the relaxed lower bound model, we used the lifting partitioning and partitioning of variables representing the product of flow and temperature. We first tested adding the lifting partitioning in the lower bound model. New variables for total area (TA) and total heat amount of heater (TQ) were introduced and partitioned through Eqs. (106)–(111). Lower limits of TA and TQ are 5590 m^2 and 11,700 KJ/s calculated from pinch analysis. Upper limits are used 30% higher values than lower limits. The results of using our lifting partitioning is shown in Table 13. They are strikingly similar because the extended elimination used 2 intervals until the end.

Next, we added partitioning of bilinear terms (Eqs. (112)–(119)) into the model to help bound contracting. The results for different forbidding methods in the bound contracting procedure with 1% tolerance gap are shown in Table 14.

The lifting partitioning increased the lower bound and helped to find the objective value satisfying 1% tolerance gap. However, after adding partitioning of variables of the product of flow and temperature, there was no improvements on the number of iterations and CPU time because more partitioned variables were added into the lower bound model and bound contracting procedure.

We tested our bilinear and nonconvex model comparing to the bilinear model, which used in the lower bound model (Eqs. (80)–(83)). The result of bilinear model with the lifting partitioning and the extended interval forbidding is shown in Table 15.

The optimum solution, presented in Fig. 11a, has an annualized cost of $1,785,239. The results are summarized in Table 16. We also show an alternative solution with a different Gap. Fig. 11b shows an alternative solution. The purpose of showing these is to point out that the problem is hard to solve, especially because there are several solutions within a small gap. We also notice in this solution, a match between stream H1 and C2 that cannot be obtained using other models, like the popular stage model (Yee and Grossmann, 1990), even with the extensions to non-isothermal mixing. Fig. 12, in turn, shows the solution when limiting splits.

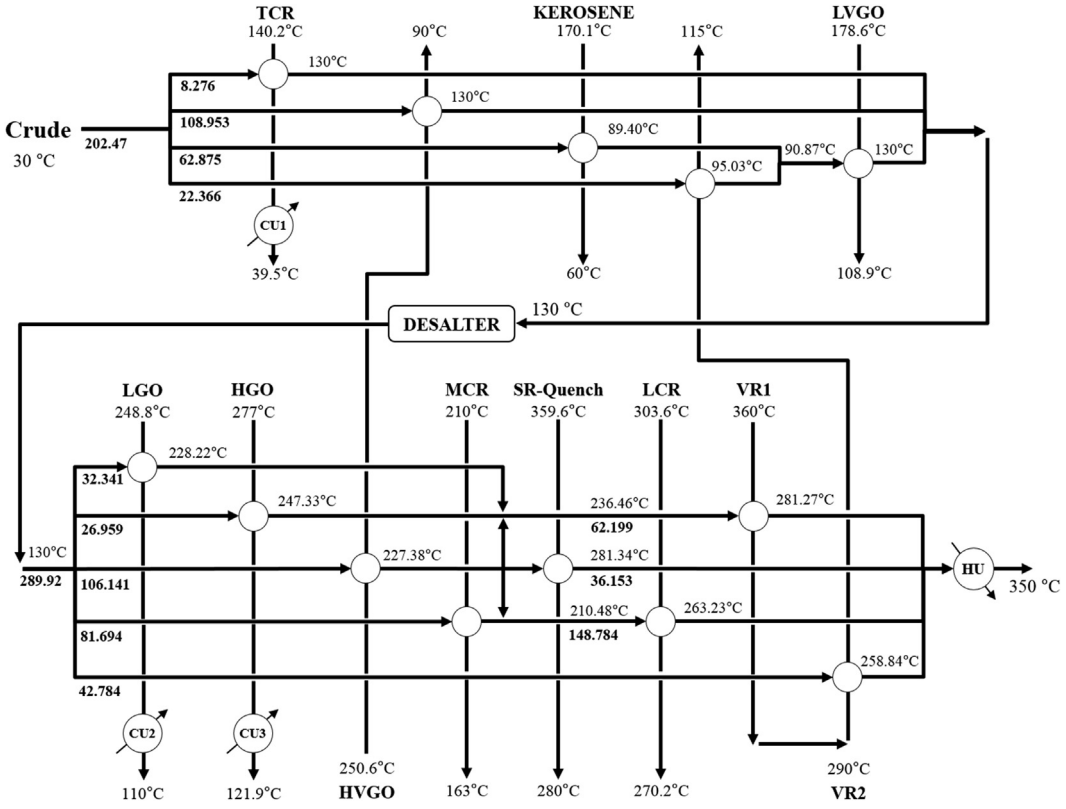

Fig. 8. The solution network for example 3.

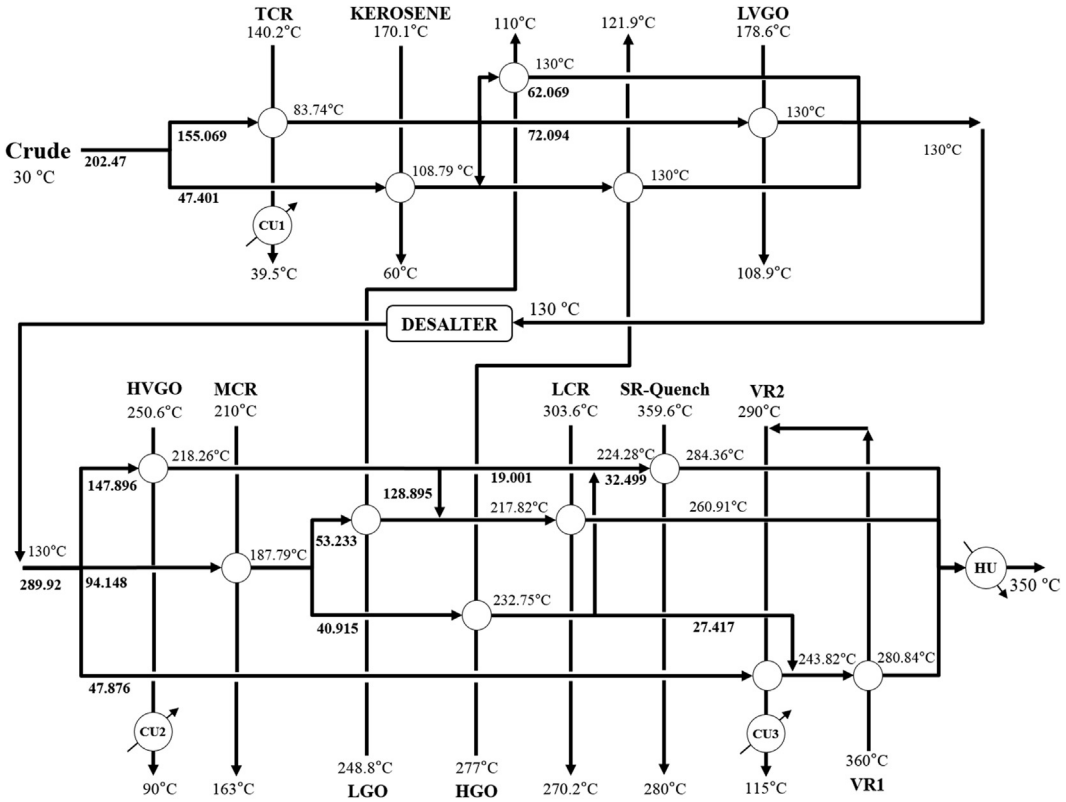

Fig. 9. The solution network with *Nsplit* = 3.

Finally, we noticed that in all the above experiments with the methodology, we reached the lower bound of the heating utility. When we run using a bound that is lower, namely 11,000, we obtained a solution in between bounds with 4.7% gap, in a time much larger than the one reported above (1 h 36 m 22 s). At this point in time, we leave for further work the investigation of what makes this example behave this way, especially in view of the fact that the following much larger examples behave so well. We

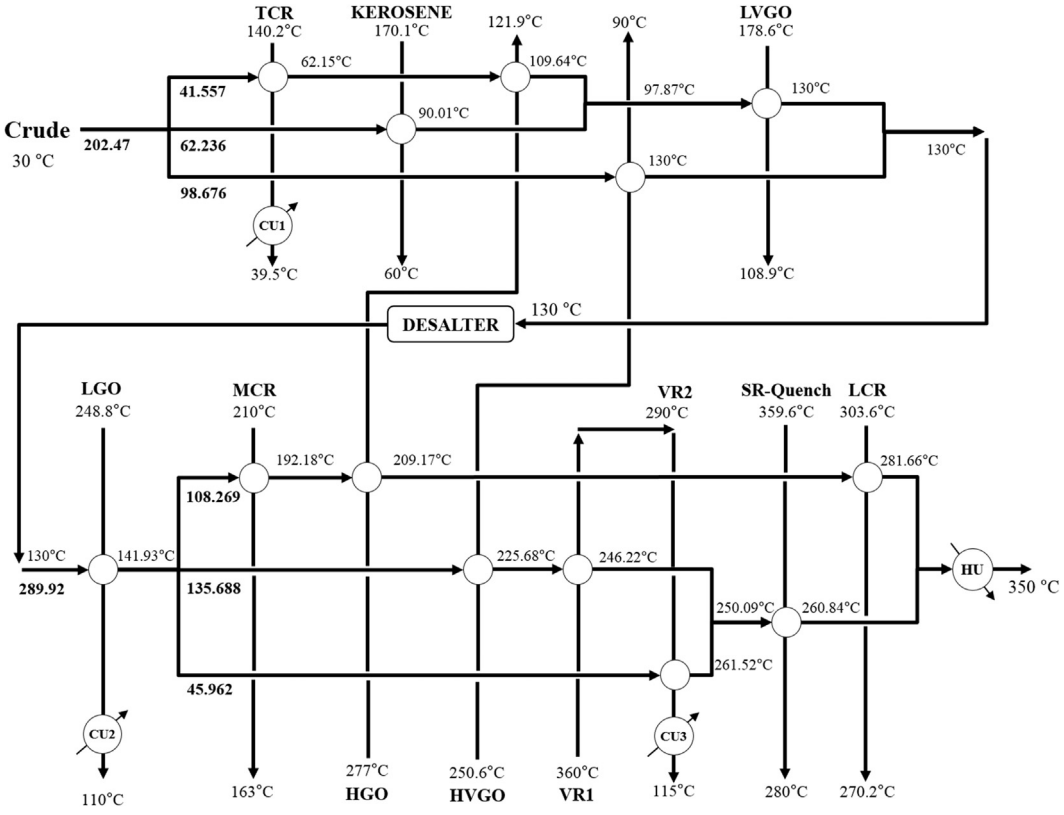

Fig. 10. The solution network with *Nsplit*=3 and *Tsplit*=1.

Table 10
Data for example 3.

Stream	Fcp [kJ/s C]	Cp [kJ/Kg °C]	T_{in} [C]	T_{out} [°C]	h [kJ/s m^2 °C]
H1	228.5	1	159	77	0.4
H2	20.4	1	267	88	0.3
H3	53.8	1	343	90	0.25
C1	93.3	1	26	127	0.15
C2	196.1	1	118	265	0.5
HU		1	500	499	0.53
CU		1	20	40	0.53

Table 11
Cost data for example 3.

Heating utility cost	100 [$/(kJ/s)]
Cooling utility cost	10 [$/−(kJ/s)]
Fixed cost for heat exchangers	250,000 [$/unit]
Variable cost for heat exchanger area	550 [$/m^2]

Table 12
Results of partitioning of ΔT and stream temperature in the lower bound model.

	# of starting intervals	Objective value ($) (upper bound)	Gap	# of iterations	# of intervals at convergence	CPU time
Single interval elimination	2	1,789,968	45%	15	2	1 h 43 m 06 s
Extended interval elimination	2	1,789,968	45%	15	2	1 h 43 m 41 s

Table 13
Results with lifting partitioning.

	# of starting intervals	Objective value ($) (upper bound)	Gap	# of iterations	# of intervals at convergence	CPU time
Single interval elimination	2	1,785,239	0.74%	11	3	6 m 58 s
Extended interval elimination	2	1,785,239	0.74%	11	3	6 m 58 s

Table 14
Results of lifting partitioning and partitioning the product of flow and temperature ($FTh_{\Pi}^{i,j,k}$).

	# of starting intervals	Objective value ($) (upper bound)	Gap	# of iterations	# of intervals at convergence	CPU time
Single interval elimination	2	1,785,239	0.74%	14	3	20 m 34 s
Extended interval elimination	2	1,785,239	0.74%	14	3	20 m 41 s

Table 15
Result of bilinear model lower bound.

# of starting intervals	Objective value (upper bound)	Gap	# of bound contraction cycles	# of intervals at convergence	CPU time
2	1,799,324	0.13%	16	4	13 m 03 s

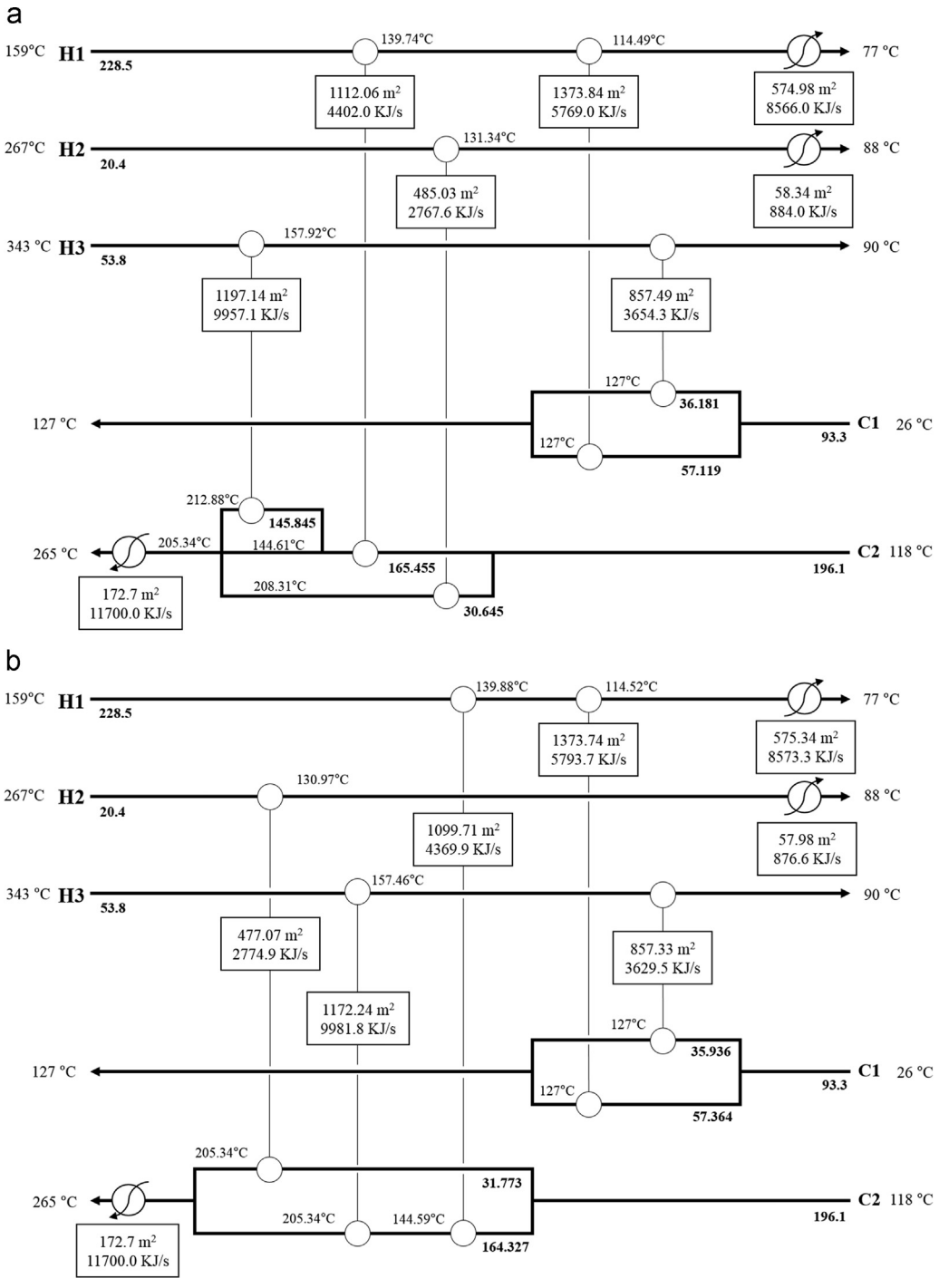

Fig. 11. The solution network for example 1. Two alternative solutions (a) Gap=0.74%, (b) Gap=0.61%.

Table 16
Summary of results for example 3a.

Total area	5,831.58 m^2
Number of exchangers	8
Heating utility	11,700 kJ/s
Cooling utility	9450 kJ/s
Final objective function (Total annual cost)	$1,785,239

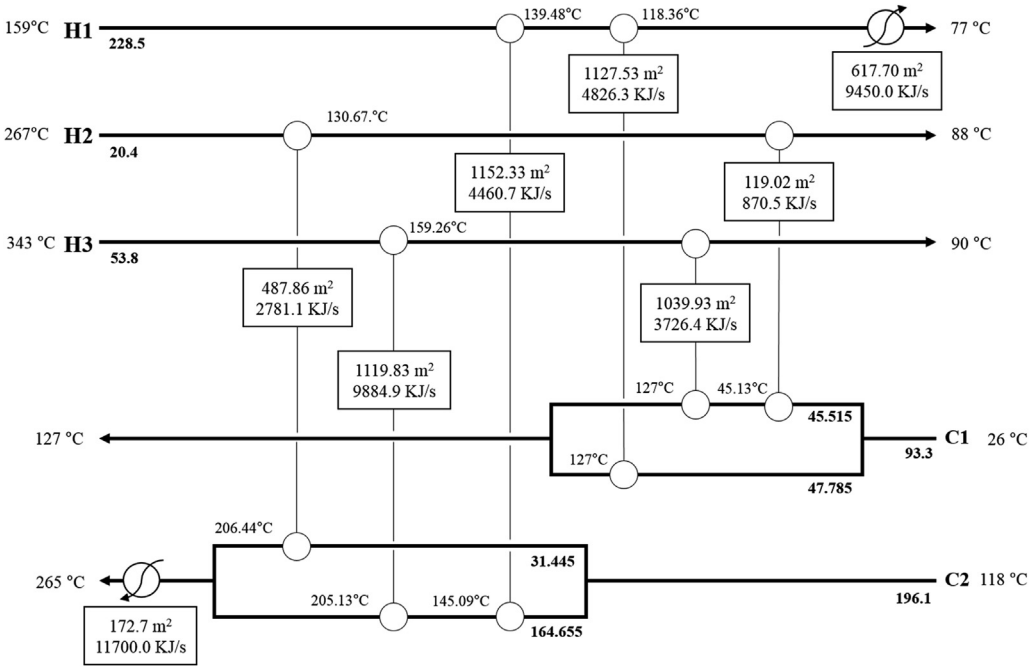

Fig. 12. The solution with forbidding bypasses, *TSPLIT*=1 and *NSPLIT*=3 (Gap=0.76%).

tested with various conditions of $\sum Q_j^{HU}$ in the lifting partitioning. We first tested with the lower *TQ* limit of 11,000 KJ/s and the upper *TQ* limit of 11,100 KJ/s in the lower bound model. We also used $\sum Q_j^{HU} \geq TQ$ instead of $\sum Q_j^{HU} = TQ$ in the lifting partitioning. Next, we fixed $\sum Q_j^{HU}$ as 11,000, 11,050, 11,100 and 11,200. In all cases, they spent much larger time than the one reported in Table 13 and identified the global optimum early and spent the rest of the time improving the lower bound.

We also note that RYSIA (our method) and ANTIGONE, but not BARON, identify the global optimum early and spend the rest of the time improving the lower bound.

9. Conclusion

We presented a new generalized superstructure model that includes multiple stream matching. This is an extension of the superstructure presented by Floudas et al. (1986) where only one match with hot and cold stream pairs was allowed. Recognizing that local solvers like DICOPT cannot obtain solutions, often rendering infeasible if no goo initial point is provided, we solve it globally using RYSIA, our bound contraction method for bilinear problems (Faria et al., 2011) extended to monotone functions by Faria et al. (2015). When applying these versions of RYSIA, we found that the lower bound model is too relaxed and therefore the bound contraction takes a long number of iterations. To fix this problem, we introduce so-called "lifting partitioning", which helps the lower bound render higher values. We compare with the bilinear reformulation and branch and bound and we present results that highlight features in the HEN that other models cannot model.

Nomenclature

Sets and indexes

i	hot process stream
j	cold process stream
k	sharing of heat exchanger (i,j)
$l1$	hot stream location
$l2$	cold stream location (in: inlet , hx-in: inlet to HX, hx-out: outlet from HX, out: outlet)
m	exchanged heat-partitioning point
$n1$	hot side temperature differences partitioning point
$n2$	cold side temperature differences partitioning point
o	flowrate partitioning point
p	area partitioning point

Positive variables

$Fh_{l1}^{i,j,k}$	heat capacity flow rate for hot stream
$fh_{k,kk}^{i,j,jj}$	heat capacity flow rate related to mixers and splitters for hot stream

$Fc_{l2}^{i,j,k}$ heat capacity flow rate for cold stream

$fc_{k,kk}^{i,i,ii}$ heat capacity flow rate related to mixers and splitters for cold stream

$Th_{l1}^{i,j,k}$ temperature for hot stream

$th_{k,kk}^{i,j,jj}$ temperature related to mixers and splitters for hot stream

$Tc_{l2}^{i,j,k}$ temperature for cold stream

$tc_{k,kk}^{j,i,ii}$ temperature related to mixers and splitters for cold stream

$FTh_{l1}^{i,j,k}$ product of $Fh_{l1}^{i,j,k}$ and $Th_{l1}^{i,j,k}$

$fth_{k,kk}^{i,j,jj}$ product of $fh_{k,kk}^{i,j,jj}$ and $th_{k,kk}^{i,j,jj}$

$FTc_{l2}^{i,j,k}$ product of $Fc_{l2}^{i,j,k}$ and $Tc_{l2}^{i,j,k}$

$ftc_{k,kk}^{j,i,ii}$ product of $fc_{k,kk}^{j,i,ii}$ and $tc_{k,kk}^{j,i,ii}$

T_H^i hot stream temperature after the last mixer

T_C^j cold stream temperature after the last mixer

$FhB_{l1}^{i,j,k,o}$ bilinear term between variable $Fh_{l1}^{i,j,k}$ and binary $vThD_{l1}^{i,j,k,o}$

$\Delta Th_{i,j,k}$ hot side temperature difference

$\Delta Tc_{i,j,k}$ cold side temperature difference

ΔT_i^{CU} cold utility temperature difference

ΔT_j^{HU} hot utility temperature difference

$Q_{i,j,k}$ heat exchanged between streams i and j for heat exchanger (i,j,k)

Q_i^{CU} heat exchanged between i and the cold utility

Q_j^{HU} heat exchanged between j and the hot utility

$A_{i,j,k}$ area of heat exchanger (i,j,k)

A_i^{CU} area of cold utility

A_j^{HU} area of hot utility

$H_{i,j,k,n1,n2}$ additional positive variable from the product of $Yh_{i,j,k,n1}$, $Yc_{i,j,k,n2}$ and $A_{i,j,k}$

$\alpha_{i,j,k}$ maximum temperature inlet to mixer

$\beta_{i,j,k}$ minimum temperature inlet to mixer

TQ total utility usage

TA total area

Binary variables

$Z_{i,j,k}$ binary variable to denote kth sharing existence of match (i and j)

Z_i^{CU} binary variable to denote existence of cold utility between hot stream i

Z_i^{CU} binary variable to denote existence of cold utility between hot stream i

$vThD_{l1}^{i,j,k}$ binary variable related to the partitioned hot stream temperature $Th_{l1}^{i,j,k}$

$Yh_{i,j,k,n1}$ binary variable related to the partitioned hot side temperature differences

$Yc_{i,j,k,n2}$ binary variable related to the partitioned cold side temperature differences

$Rh_{l1}^{i,j,k}$ binary variable to denote the existence of hot stream

$rh_{k,kk}^{i,j,jj}$ binary variable to denote the existence of hot stream

$Rc_{l2}^{i,j,k}$ binary variable to denote the existence of cold stream

$rc_{k,kk}^{j,i,ii}$ binary variable to denote the existence of cold stream

$pHup_{k,kk}^{i,j,jj}$ binary variable to denote the maximum temperature of hot stream inlet to mixer

$pHlo_{k,kk}^{i,j,jj}$ binary variable to denote the minimum temperature of hot stream inlet to mixer

$Ymh_{i,j,jj}$ binary variable to denote the existence of the recycle for hot stream

$Ymc_{j,i,ii}$ binary variable to denote the existence of the recycle for cold stream

Sh_i binary variable to denote existence of a split for inlet hot stream i

$Shh_{i,j,k}$ binary variable to denote existence of a split for outlet stream from heat exchanger

vTQ_m binary variable related to the partitioned total utility usage

vTA_p binary variable related to the partitioned total area

$vFTh_{l1}^{i,j,k}$ binary variable related to the partitioned $FTh_{l1}^{i,j,k}$

$vFTc_{l2}^{i,j,k}$ binary variable related to the partitioned $FTc_{l2}^{i,j,k}$

$vfth_{k,kk}^{i,j,jj}$ binary variable related to the partitioned $fth_{k,kk}^{i,j,jj}$

$vftc_{k,kk}^{i,j,jj}$ binary variable related to the partitioned $ftc_{k,kk}^{i,j,jj}$

$ih_{i,j,k}$ binary variable to denote existence of inlet streams from other exchangers for hot stream

$ic_{i,j,k}$ binary variable to denote existence of inlet streams from other exchangers for cold stream

$bh_{i,j,k}$ binary variable to denote existence of outlet streams going to other exchangers for hot stream

$bc_{i,j,k}$ binary variable to denote existence of outlet streams going to other exchangers for cold stream

Parameters

T_i^{HIN} inlet temperature of hot stream i

T_i^{HOUT} outlet temperature of hot stream i

T_j^{CIN} inlet temperature of cold stream j

T_j^{COUT} outlet temperature of cold stream j

$T_{OUT,CU}$ outlet temperature from the cold utility

$T_{IN,CU}$ inlet temperature from the cold utility

$T_{OUT,HU}$ outlet temperature from the hot utility

$T_{IN,HU}$ inlet temperature from the hot utility

F_i specific inlet heat capacity flow rate of hot stream i

F_j specific inlet heat capacity flow rate of cold stream j

$U_{i,j,k}$ overall heat transfer coefficient for heat exchanger (i,j,k)

U_i^{CU} overall heat transfer coefficient for cold utility

U_j^{HU} overall heat transfer coefficient for hot utility

$HU\text{cost}$ hot utility cost

$CU\text{cost}$ cold utility cost

$ThD_{l1}^{i,j,k,o}$ discrete point of the partitioned temperature of hot stream $Th_{l1}^{i,j,k}$

$\Delta ThD_{i,j,k,n1}$ discrete point of temperature differences in hot side of heat exchanger (i,j,k)

$\Delta TcD_{i,j,k,n2}$ discrete point of temperature differences in cold side of heat exchanger (i,j,k)

Γ large parameter in Big M constraints. It is usually slightly larger than the maximum number of the variable for which a zero-one variable is created.

$NSplit_i$ number of branches of hot stream i

$TSplit_i$ number of times hot stream i splits

$TMMax_{i,j,k}$ maximum difference of temperatures allowed in a mixer

$DT_{i,j,k}$ logarithmic mean temperature differences

$\hat{D}_{i,j,k,l}$ discretized values of the logarithmic mean temperature differences

TQD discrete point of the partitioned total utility usage

TAD discrete point of the partitioned total area

$dFTh_{l1}^{i,j,k}$ discrete point of the partitioned $FTh_{l1}^{i,j,k}$
$dFTc_{l2}^{i,j,k}$ discrete point of the partitioned $FTc_{l2}^{i,j,k}$
$dfth_{k,kk}^{i,j,jj}$ discrete point of the partitioned $fth_{k,kk}^{i,j,jj}$
$dftc_{k,kk}^{i,j,jj}$ discrete point of the partitioned $ftc_{k,kk}^{i,j,jj}$

References

Brooke, A., Kendrick, D., Meeraus, D., Raman, R., 2007. GAMS – A User Guide. GAMS Development Corporation, Washington D. C.

Björk, K., Weterlund, T., 2002. Global optimization of heat exchanger network synthesis problems with and without the isothermal mixing assumption. Comput. Chem. Eng. 26, 1581–1593.

Cerda, J., 1980. Transportation Models for the Optimal Synthesis of Heat Exchanger Networks. Carnegie-Melon University, Pittsburgh.

Chen, J.J.J., 1987. Comments on improvements on a replacement for the logarithmic mean. Chem. Eng. Sci. 42, 2488–2489.

Faria, D., Bagajewicz, M., 2011a. Novel bound contraction procedure for global optimization of bilinear MINLP problems with applications to water management problems. Comput. Chem. Eng. 35, 446–455.

Faria, D., Bagajewicz, M., 2011b. A new approach for global optimization of a class of MINLP Problems with applications to water management and pooling problems. AIChE J. 58 (8), 2320–2335.

Faria, D., Bagajewicz, M., 2011c. Global optimization of water management problems using linear relaxations and bound contraction methods. Ind. Eng. Chem. Res. 50 (7), 3738–3753.

Faria, D.C., Kim, S.Y., Bagajewicz, M.J., 2015. Global optimization of the stage-wise superstructure model for heat exchanger networks. Ind. Eng. Chem. Res. 54 (5), 1595–1604.

Floudas, C.A., Ciric, A.R., Grossmann, I.E., 1986. Automatic synthesis of optimum heat exchanger network configurations. AIChE J. 32 (2), 276–290.

Furman, K.C., Sahinidis, N.V., 2002. A critical review and annotated bibliography for heat exchanger network synthesis in the 20th century. Ind. Eng. Chem. Res. 41 (10), 2335–2370.

Huang, K.F., Karimi, I.A., 2013. Simultaneous synthesis approaches for cost-effective heat exchanger networks. Chem. Eng. Sci. 98, 231–245.

Manousiouthakis, V., Sourlas, D., 1992. A global optimization approach to rationally constrained rational programming. Chem. Eng. Commun. 118, 127–147.

Nguyen, D.Q., Barbaro, A., Vipanurat, N., Bagajewicz, M.J., 2010. All-at-once and step-wise detailed retrofit of heat exchanger networks using an MILP model. Ind. Eng. Chem. Res. 49, 6080–6103.

Paterson, W.R., 1984. A replacement for the logarithmic mean. Chem. Eng. Sci. 39, 1635–1636.

Viswanathan, J., Grossmann, I.E., 1990. A combined penalty function and outer approximation method for MINLP Optimization. Comput. Chem. Eng. 14, 769–782.

Yee, T.F., Grossmann, I.E., 1990. Simultaneous optimization model for heat integration – II. heat exchanger network synthesis. Comput. Chem. Eng. 14, 1165–1184.